European Journal of Medicinal Chemistry 74 (2014) 562–573

Contents lists available at ScienceDirect

European Journal of Medicinal Chemistry

journal homepage: http://www.elsevier.com/locate/ejmech

Original article

Development of potent and selective *Plasmodium falciparum* calcium-dependent protein kinase 4 (*Pf*CDPK4) inhibitors that block the transmission of malaria to mosquitoes

Rama Subba Rao Vidadala [a], Kayode K. Ojo [b], Steven M. Johnson [a], Zhongsheng Zhang [c], Stephen E. Leonard [a], Arinjay Mitra [a], Ryan Choi [b], Molly C. Reid [b], Katelyn R. Keyloun [b], Anna M.W. Fox [b], Mark Kennedy [d], Tiffany Silver-Brace [d], Jen C.C. Hume [d], Stefan Kappe [d,e], Christophe L.M.J. Verlinde [c], Erkang Fan [c], Ethan A. Merritt [c], Wesley C. Van Voorhis [b,e,f,**], Dustin J. Maly [a,*]

[a] Department of Chemistry, University of Washington, Seattle, WA 98195-1700, USA
[b] Division of Allergy and Infectious Diseases, Department of Medicine, University of Washington, Seattle, WA, USA
[c] Department of Biochemistry, University of Washington, Seattle, WA, USA
[d] Seattle Biomedical Research Institute, Seattle, WA, USA
[e] Departments of Global Health, University of Washington, Seattle, WA, USA
[f] Departments of Microbiology, University of Washington, Seattle, WA, USA

ARTICLE INFO

Article history:
Received 19 October 2013
Received in revised form
23 December 2013
Accepted 26 December 2013
Available online 11 January 2014

Keywords:
Plasmodium falciparum
*Pf*CDPK4
*Pf*CDPK1
Pyrazolopyrimidine
Exflagellation

ABSTRACT

Malaria remains a major health concern for a large percentage of the world's population. While great strides have been made in reducing mortality due to malaria, new strategies and therapies are still needed. Therapies that are capable of blocking the transmission of *Plasmodium* parasites are particularly attractive, but only primaquine accomplishes this, and toxicity issues hamper its widespread use. In this study, we describe a series of pyrazolopyrimidine- and imidazopyrazine-based compounds that are potent inhibitors of *Pf*CDPK4, which is a calcium-activated *Plasmodium* protein kinase that is essential for exflagellation of male gametocytes. Thus, *Pf*CDPK4 is essential for the sexual development *of Plasmodium* parasites and their ability to infect mosquitoes. We demonstrate that two structural features in the ATP-binding site of *Pf*CDPK4 can be exploited in order to obtain potent and selective inhibitors of this enzyme. Furthermore, we demonstrate that pyrazolopyrimidine-based inhibitors that are potent inhibitors of the *in vitro* activity of *Pf*CDPK4 are also able to block *Plasmodium falciparum* exflagellation with no observable toxicity to human cells. This medicinal chemistry effort serves as a valuable starting point in the development of safe, transmission-blocking agents for the control of malaria.

1. Introduction

Malaria is a major health concern for much of the tropics and subtropics [1–4]. Malaria infections are transmitted to humans by the bite of female *Anopheles* mosquitoes. Four *Plasmodium* species, *Plasmodium falciparum*, *Plasmodium vivax*, *Plasmodium malariae*, and *Plasmodium ovale* are responsible for the majority of human infections. Recently, a fifth species, *Plasmodium knowlesi*, which was previously thought to infect only non-human primates, has been found to be adapted to spread from human-to-mosquito-to-human in Malaysia [5,6]. Although insecticide-treated bed nets, vector control, and effective chemotherapies have resulted in reduced mortality, an estimated 1,238,000 people still die of malaria every year [7]. While efforts are underway to effectively

Abbreviations: ACT, artemisinin combination therapy; ATP, adenosine triphosphate; Boc, *tert*-butyloxycarbonyl; CAMKII, Ca^{2+}/calmodulin-dependent protein kinase II; CDPK1, calcium-dependent protein kinase 1; *Cp*CDPK1, *Cryptosporidium parvum* CDPK1; DIAD, diisopropyl azodicarboxylate; DME, dimethoxyethane; EC_{50}, half maximal effective concentration; GI_{50}, half maximal growth inhibition; IC_{50}, half maximal inhibitory concentration; IGF1R, insulin-like growth factor 1 receptor; *Pf*CDPK1, *Plasmodium falciparum* CDPK1; *Pf*CDPK4, *Plasmodium falciparum* CDPK4; TBDMS, *tert*-butyldimethylsilyl; *Tg*CDPK1, *Toxoplasma gondii* CDPK1.

* Corresponding author. Tel.: +1 206 543 1653; fax: +1 206 685 7002.
** Corresponding author. Division of Allergy and Infectious Diseases, Department of Medicine, University of Washington, Seattle, WA, USA. Tel.: +1 206 543 2447; fax: +1 206 616 4898.
E-mail addresses: wesley@uw.edu (W.C. Van Voorhis), maly@chem.washington.edu (D.J. Maly).

0223-5234/$ – see front matter © 2014 Elsevier Masson SAS. All rights reserved.
http://dx.doi.org/10.1016/j.ejmech.2013.12.048

control *Anopheles* mosquito populations, this task remains a major challenge. In order to control and eradicate malaria, it will be necessary to develop new methods of reducing parasite transmission, especially in light of increasing mosquito resistance to insecticide-treated bed nets [8].

Currently available therapeutics mainly target the erythrocytic (asexual) stage of malaria, but not gametocytes (sexual forms) [9]. As circulating gametocytes maintain the capacity to infect mosquitoes for weeks after therapy, the lack of transmission-blocking activity of these therapies hinders malaria control [10,11]. While primaquine and artemisinin combination therapy (ACT) possess anti-gametocyte activity, these drugs are not ideal for preventing malaria transmission to mosquitoes. Artemisinin only kills immature gametocytes, while primaquine only kills mature gametocytes [12]. Although extended primaquine treatment can effectively eradicate gametocytes from the blood, many patients suffer GI intolerance and hemolysis results in patients with glucose-6-phosphate dehydrogenase deficiency [10,13]. For these reasons, a number of new transmission blocking strategies have been explored [13–15].

The life cycle stages of malaria parasites alternate between human and mosquito hosts (Fig. 1) [15]. Female *Anopheles* mosquitoes transmit sporozoites to humans, where asexual reproduction produces merozoites. A subset of merozoites develop into gametocytes, which upon the bite of a mosquito can be taken up with blood and allowed to mature in the mosquito midgut. Inhibition of specific calcium-dependent processes can block this maturation and the eventual formation of mature sporozoites in the mosquito salivary glands, which would otherwise be transmitted when the mosquito next bites a human (Fig. 1).

Precise control over malaria life cycle stages is coordinated through intricate signal transduction pathways that are regulated by a number of secondary messengers. One such secondary messenger is calcium, which is involved in important life cycle events, such as host cell invasion, protein secretion, gliding motility, and exflagellation [16]. In addition to other enzymes, calcium release in *Plasmodium* activates a family of plant- and apicomplexan-specific kinases called the calcium-dependent protein kinases (CDPKs) [17,18]. Binding of calcium to this family of kinases releases an auto-inhibitory domain interaction, increasing the catalytic activity of the kinase domain, which results in the phosphorylation of numerous cellular substrates [19]. *Plasmodium* CDPKs are attractive drug targets because they are unique to plants and apicomplexans. Furthermore, these kinases are involved in a number of important *Plasmodium* life cycle processes, including various steps involved in transmission.

While all of the functions of *Plasmodium* CDPKs have not been fully characterized, their roles in several important calcium-regulated processes have been described. *P. falciparum* CDPK1 (*Pf*CDPK1) has been reported to be involved in the regulation of parasite motility and in controlling zygote development and transmission [20,21]. *P. falciparum* CDPK5 (*Pf*CDPK5) has been implicated in the regulation of malaria parasite egress from erythrocytes, and *Plasmodium berghei* CDPK3 (*Pb*CDPK3) is required for ookinete gliding motility and invasion of mosquito midguts [22,23]. Genetic experiments have demonstrated that *P. berghei* CDPK4 (*Pb*CDPK4), and presumably the homologous *Pf*CDPK4, is essential for microgamete (male gametocytes) exflagellation and sexual stage development in the mosquito [24]. Furthermore, we have previously reported that potent and selective *Pf*CDPK4 inhibitors are capable of blocking *Plasmodium* microgamete exflagellation, thus disrupting malaria transmission [25,26]. Expression in *P. falciparum* of an exogenous drug-resistant *Pf*CDPK4 mutant led to a 12-fold reduction in sensitivity to a *Pf*CDPK4 inhibitor in exflagellation assays [26]. Therefore, *Pf*CDPK4 has been validated genetically and pharmacologically as a promising drug target for the development of transmission blocking therapies. Here, we report a detailed molecular analysis of the requirements for potent and selective *Pf*CDPK4 inhibition. We show that certain structural features in *Pf*CDPK4's ATP-binding site can be exploited to obtain highly potent and selective inhibitors. Furthermore, we demonstrate that pyrazolopyrimidine-based inhibitors containing diverse functional groups, which inhibit the catalytic activity of *Pf*CDPK4 *in vitro*, are effective at blocking the exflagellation of *P. falciparum*. These studies suggest *Pf*CDPK4 is an attractive target for the development of malaria transmission-blocking therapy, both for its essential role in exflagellation and due to its pharmacological tractability.

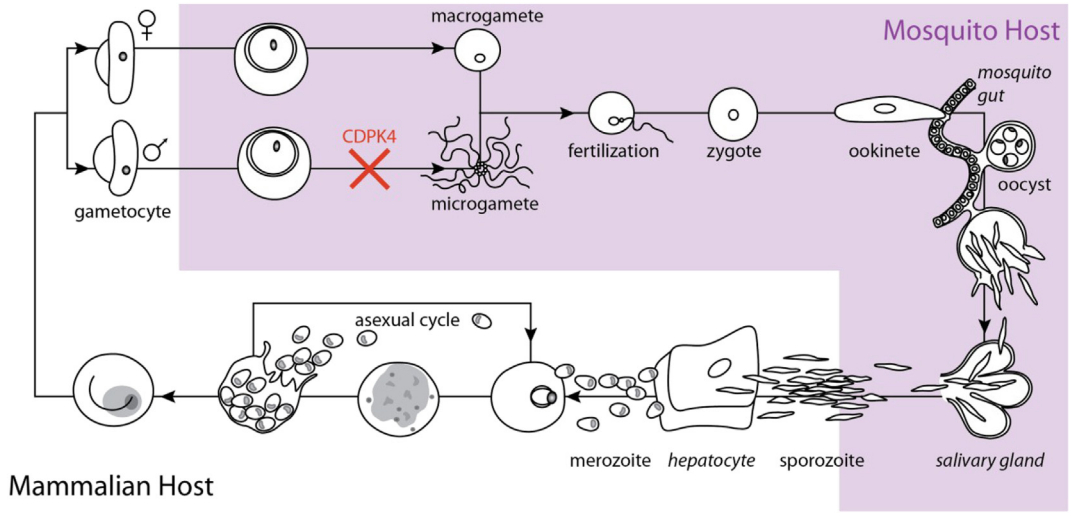

Fig. 1. Diagram of the Malaria parasite life cycle. Asexual mammalian-host stages are shown in white and life cycle stages that occur in the mosquito are shown in light purple. A subset of merozoites differentiate into male and female gametocytes, which are ingested by female mosquitoes upon biting an infected human. In the mosquito gut, male gametocytes divide into flagellated microgametes, which escape red blood cells (exflagellation) and swim to the macrogamete, resulting in fertilization. The resultant motile zygote forms an ookinete, which moves across the mosquito gut to form oocysts. Oocysts rupture to form sporozoites that mature in mosquito salivary glands and can be injected into humans by mosquito bites. In humans, replication *via* the asexual life cycle occurs. Inhibitors of *Pf*CDPK4, block transmission by preventing exflagellation. (For interpretation of the references to color in this figure legend, the reader is referred to the web version of this article.)

Table 1
Enzymatic assay (IC_{50}) results for compounds with variable R_1 substructures (**5**–**35**) across the R_2 series **a** and **b**. All results are the averages of at least three assays. *Tg*CDPK1 IC_{50} values for a number of compounds have previously been reported [28,29].

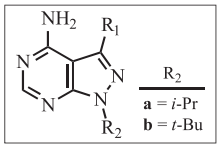

	R_1	R_2	IC_{50} (μM)			
			*Pf*CDPK4	*Tg*CDPK1	*Pf*CDPK1	Src
5		b	0.40	0.004	0.34	0.13
6		b	1.5	0.004	>3	0.18
7		a	>3	0.96	>3	N/T
8		a	0.34	0.011	0.47	1.5
9		a	0.54	0.009	1.7	1.2
10		a b	0.23 0.57	0.003 0.013	0.31 1.2	0.29 0.52
11		b	0.094	0.002	0.29	2.1
12	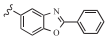	b	>3	0.12	0.27	N/T
13		a b	>3 >3	2.2 0.40	2.9 >3	N/T N/T
14		a b	>3 0.44	0.13 0.031	N/T 2.44	8.8 2.2
15		a b	0.14 0.18	0.005 0.015	0.38 0.43	0.065 0.12
16		a b	0.041 0.14	0.006 0.020	0.21 0.67	0.58 2.0
17		a b	0.43 0.077	0.005 0.033	1.3 2.4	0.55 2.2
18		a	0.55	0.010	0.37	0.63
19	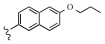	a	0.53	0.003	0.66	0.31
20	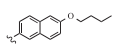	a	0.31	0.0009	0.16	0.78
21	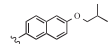	a b	1.2 >3	0.005 0.20	0.28 2.9	N/T 1.1
22	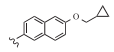	a	0.080	0.004	0.036	0.050
23	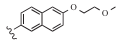	a	0.076	0.004	0.053	0.38
24	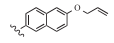	a	0.019	0.006	0.036	0.20

Table 1 (*continued*)

	R_1	R_2	IC_{50} (μM)			
			*Pf*CDPK4	*Tg*CDPK1	*Pf*CDPK1	Src
25	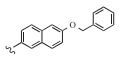	a	0.51	0.0008	0.096	0.043
26	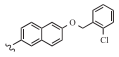	a	>3	0.010	0.48	0.28
27	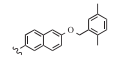	a	>3	0.14	2.3	0.88
28	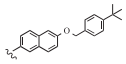	a	0.44	0.015	0.047	0.13
29		a b	0.17 >3	0.024 0.031	1.4 N/T	0.20 4.1
30		a	0.012	0.002	0.19	1.1
31		a	0.22	0.059	>3	N/T
32	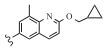	a	>3	0.35	>3	N/T
33	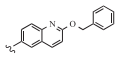	a	0.21	0.0009	0.075	0.025
34	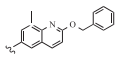	a	>3	0.40	>3	4.1
35	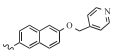	a	0.18	0.016	0.22	0.90

2. Results and discussion

2.1. Molecular design

We have generated and characterized a number of pyrazolopyrimidine-based inhibitors that selectively target *Toxoplasma gondii* CDPK1 (*Tg*CDPK1) and *Cryptosporidium parvum* CDPK1 (*Cp*CDPK1) [27–30]. These kinases contain an enlarged ATP-binding pocket due to the presence of a glycine at a conserved structural feature called the gatekeeper residue. As mammalian kinases contain gatekeeper residues larger than glycine, this unique structural element can be targeted to obtain highly selective ATP-competitive inhibitors. Through iterative rounds of synthesis and testing, we have identified aryl substituents displayed from the C-3 position of the pyrazolo[2,3-*d*]pyrimidine scaffold that optimally complement the ATP-binding pockets of *Tg*CDPK1 and *Cp*CDPK1 (*Tg*/*Cp*CDPK1). Many of these inhibitors are highly selective for *Tg*/*Cp*CDPK1 over mammalian kinases. While *Pf*CDPK4 contains a serine rather than a glycine at the gatekeeper position, the rarity of mammalian kinases with a gatekeeper residue this small raises the possibility that highly selective inhibitors can be developed for this kinase as well. Furthermore, during our efforts to target *Tg*/*Cp*CDPK1 we identified an additional region of the ATP-binding site that can be exploited by inhibitors that target these kinases [30]. This structural feature, which is located in the ribose pocket of the ATP-binding site, works in concert with the gatekeeper position to allow certain bulky C-3 substituents to be specifically accommodated in the ATP-binding sites of *Tg*/*Cp*CDPK1. Due to the high degree of sequence homology in the CDPK family, we hypothesized that we could develop inhibitors that exploit a similar pair of interactions in *Pf*CDPK4.

The core scaffold of pyrazolo[2,3-*d*]pyrimidine inhibitors make similar hydrophobic and hydrogen-bonding contacts as the

adenine ring of ATP [31]. Substituents displayed from the N-1 position (R_2) project into the solvent-exposed ribose pocket. C-3 substituents (R_1) occupy the hydrophobic pocket adjacent to the gatekeeper residue. To determine the optimal substituents that complement the hydrophobic pocket next to the serine gatekeeper of *Pf*CDPK4, we first generated and tested a series of inhibitors that contain either an *i*-Pr- or *t*-Bu-group at the R_2 position and highly variable aryl substituents at the C-3 position (R_1) (Table 1). A second series of inhibitors that contain optimal R_1 substituents and diverse alkyl substituents displayed from the N-1 position (R_2) were next investigated (Table 2). Finally, a series of inhibitors in which the pyrazolopyrimidine core was replaced with an imidazopyrazine scaffold was also generated and tested (Table 3).

2.2. Synthesis of PfCDPK4 inhibitors

Several synthetic strategies were used to generate inhibitors based on a pyrazolo[2,3-*d*]pyrimidine scaffold. The synthetic route shown in Scheme 1 was used to generate inhibitors with *i*-Pr- or *t*-Bu-groups at the R_2 position (series **a** and **b**). All compounds in Table 1 were generated from halogen-containing intermediates **1** and **2**, which were made using previously described synthetic routes [29,32]. The aryl substituents of compounds **7a**–**35a** and **5b**–**29b** were introduced at the C-3 positions of **1** and **2** *via* palladium-catalyzed Suzuki–Miyaura coupling reactions with appropriate aryl boronic acids and boronate esters. Boronic acids or esters that were not commercially available were prepared using a palladium-mediated cross coupling between aryl bromides and bis(pinacolato)diboron. Compounds **18a**–**28a** and **21b**, which contain extended 6-alkoxy- and 6-benzyloxynaphtyl groups at the C-3 position, were generated by first performing a Suzuki–Miyaura coupling between 6-TBDMS-naphthalene-2-boronic acid and **1** and **2**, followed by alkylation of the deprotected naphthols **3** and **4** with alkyl and benzyl halides (Scheme 1). Compounds containing variable groups at the R_2 position (Table 2) were generated by alkylating 3-iodo-1*H*-pyrazolo[3,4-*d*]pyrimidin-4-amine with alkyl halides, or alkyl mesylates, followed by Suzuki–Miyaura coupling to R_1-boronic acids or boronate pinacol esters (Scheme 2). 4-Piperidinylmethylene- and 3-azetidinemethylene-containing compounds (**15j**, **16j**, **17g**, **17j**, **19j**, **20j**, **21j**, **22j**, **24j**, **25j**, **29j**, **30j**, **33j**, **34j**, **36j**, and **37j**) were generated by alkylating 3-iodo-1*H*-pyrazolo[3,4-*d*]pyrimidin-4-amine with *N*-Boc-4-piperidinemethanol or *N*-Boc-3-azetidinemethanol mesylates (Scheme 3). The alkylated intermediates were then deprotected with 50% TFA. After Boc deprotection, alkylation or acetylation was performed to generate analogs containing **h**, **i**, **k**, and **l** R_2 groups.

Imidazo[1,5-*a*]pyrazine-based inhibitors (Table 3) were prepared using the procedure shown in Scheme 4 [33,34]. R_2 substituents were introduced by acylating 3-(chloropyrazin-2-yl) methanamine with appropriate carboxylic acids, followed by cyclization with $POCl_3$. After iodinating the scaffold with NIS and aminolysis in isopropanol, R_1 substituents were then introduced at the C-1 position *via* palladium-mediated Suzuki–Miyaura couplings with commercially available boronic acids. Piperidine-containing compound **43j** was generated by removing the CBZ protecting group from intermediate **38** with HCl. Reductive amination of **43j** with formaldehyde produced compound **43k**. Detailed procedures and characterization data for all compounds are presented in the Supporting information.

2.3. In vitro activity assays

All of the inhibitors generated were tested for their ability to inhibit recombinant *Pf*CDPK4 *in vitro*. The catalytic activity of *Pf*CDPK4 was determined using a luminescence-based assay that

Table 2
Enzymatic assay (IC_{50}) results for compounds with variable R_2 substructures (**c**–**u**) across the R_1 series containing 2-naphthyl, 6-alkoxy-2-naphthyl or 2-alkoxy-6-quinilino R_1 substituents. All results are the averages of at least three assays. *Tg*CDPK1 IC_{50} values for a number of compounds have previously been reported [28,29].

R_1	R_2	IC_{50} (μM)			
		*Pf*CDPK4	*Tg*CDPK1	*Pf*CDPK1	Src
17	c	0.039	0.002	0.18	5.6
	d	0.053	0.004	0.45	>10
	e	0.084	0.002	>3	0.81
	f	0.037	0.006	1.4	1.6
	g	0.015	0.003	0.47	>10
	h	0.037	0.006	0.96	>10
	i	0.039	0.004	1.0	1.1
	j	0.004	0.002	0.14	>10
	k	0.009	0.002	0.12	>10
	l	0.063	0.010	1.2	>10
	m	0.007	0.001	0.11	3.3
	n	0.009	0.002	0.11	5.2
	o	0.090	0.002	0.66	N/T
	p	0.044	0.002	0.83	N/T
	q	0.014	0.0008	0.32	>10
	r	0.057	0.010	0.48	0.63
15	e	0.041	0.009	0.18	N/T
	j	0.015	0.002	0.066	>10
	o	0.16	0.002	0.66	N/T
	p	0.11	0.002	0.53	N/T
	t	2.5	0.073	>3	N/T
16	j	0.004	0.004	0.23	>10
19	j	0.021	0.002	0.20	>10
20	j	0.031	0.003	0.15	>10
21	j	0.058	0.003	0.18	>10
	k	0.10	0.003	0.12	3.8
22	j	0.009	0.001	0.074	>10
24	j	0.015	0.003	0.15	>10
25	j	0.030	0.002	0.027	3.1
29	j	0.11	0.005	1.1	>10
	k	0.27	0.060	N/T	N/T
	o	0.84	0.008	>3	N/T
30	j	0.002	0.003	0.066	>10
	p	0.030	0.002	0.89	>10
	u	0.004	0.001	0.32	>10

(*continued on next page*)

Table 2 (*continued*)

R_1		R_2	IC_{50} (μM)			
			*Pf*CDPK4	*Tg*CDPK1	*Pf*CDPK1	Src
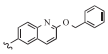	**33**	**j** 	0.012	0.003	0.005	>10
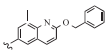	**34**	**j** 	0.072	0.010	0.053	>10
	**35**	**e** 	0.26	0.17	2.7	N/T
		f 	0.31	0.24	>3	N/T
	**36**	**j** 	>3	0.50	0.48	N/T
	**37**	**j** 	0.002	0.001	0.072	>10

measures the consumption of ATP in the presence of a peptide substrate [27]. *Pf*CDPK4 efficiently phosphorylates Syntide 2, which is a substrate for mammalian CAMKII. All assays were performed at *Pf*CDPK4's K_m for ATP (10 μM) and in the presence of 2 mM $CaCl_2$. Many of the compounds were also tested against *Tg*CDPK1, *Pf*CDPK1, and the mammalian tyrosine kinase Src. The ATP-binding sites of *Tg*CDPK1 and *Pf*CDPK1 are very similar to that of *Pf*CDPK4 in almost all of the positions predicted to interact with pyrazolopyrimidine-based inhibitors, except, most notably, the gatekeeper residue (Fig. 2). *Tg*CDPK1's glycine gatekeeper residue is smaller than *Pf*CDPK4's serine, while *Pf*CDPK1's threonine gatekeeper residue is larger. By comparing the relative sensitivities of these three CDPKs to analogs with variable R_1 substituents, the relative contribution of the gatekeeper residue to inhibitor potency can be assessed (Fig. 2). The tyrosine kinase Src was selected as a

Table 3
Enzymatic assay (IC_{50}) results for imidazo[1,5-*a*]pyrazine inhibitors. All results are the averages of at least three assays. N/T = not tested.

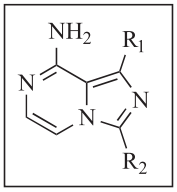

R_1		R_2	IC_{50} (μM)			
			*Pf*CDPK4	*Tg*CDPK1	*Pf*CDPK1	Src
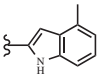	**39**	b	0.37	0.002	1.1	>10
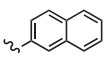	**40**	a	0.091	0.004	0.16	N/T
		b	0.018	0.003	0.061	1.3
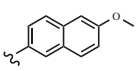	**41**	b	0.065	0.004	0.067	6.1
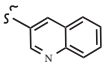	**42**	b	0.24	0.024	0.95	>10
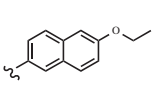	**43**	a	0.33	0.078	0.38	N/T
		b	0.13	0.004	0.20	3.9
		j	0.030	0.010	N/T	>10
		k	0.028	0.018	0.20	>10

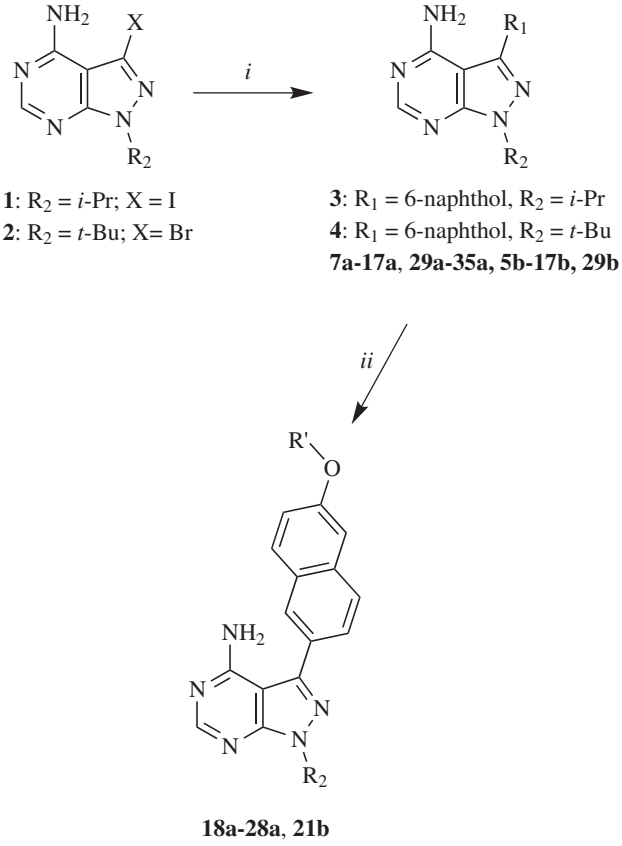

Scheme 1. General synthetic procedures for compound series **7a**–**35a** and **5b**–**29b**. *i*) Na_2CO_3, $Pd(PPh_3)_4$, boronic acid or boronate pinacol ester, H_2O/DME, 80 °C; *ii*) R′-halide, K_2CO_3, DMF, room temperature or 80 °C.

mammalian "off-target" counter-screen because it contains one of the smallest gatekeeper residues, threonine, present in humans, and was one of the original kinase targets for which pyrazolo[2,3-*d*] pyrimidine inhibitors were developed [35,36].

2.4. In vitro inhibition of recombinant *Pf*CDPK1 and *Pf*CDPK4

We first explored pyrazolopyrimidine inhibitors with large R_1 substructures (Table 1), such as substituted phenyls, indazoles, indoles, naphthyls, and quinolones, because these moieties are directed towards the gatekeeper residue and are likely to impart selectivity for *Pf*CDPK4 over mammalian kinases with bulkier residues at this position. Consistent with the hydrophobic pocket adjacent to the serine gatekeeper residue of *Pf*CDPK4 being fairly permissive, 26 out of 38 analogs in Table 1 have an IC_{50} of less than 1 μM for this enzyme. However, some R_1 substituents, such as 3-

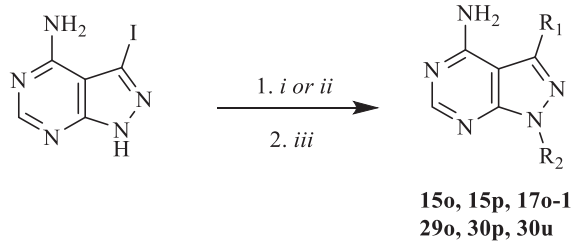

Scheme 2. General synthetic procedures for compound with variable R_2 groups. *i*) R_2-halide or R_2-mesylate, K_2CO_3, DMF, 80 °C; or *ii*) R_2-halide or R_2-mesylate, Cs_2CO_3, DMF, 80 °C; *iii*) Na_2CO_3, $Pd(PPh_3)_4$, R_1-boronic acid or R_1-boronate pinacol ester, H_2O/DME, 80 °C.

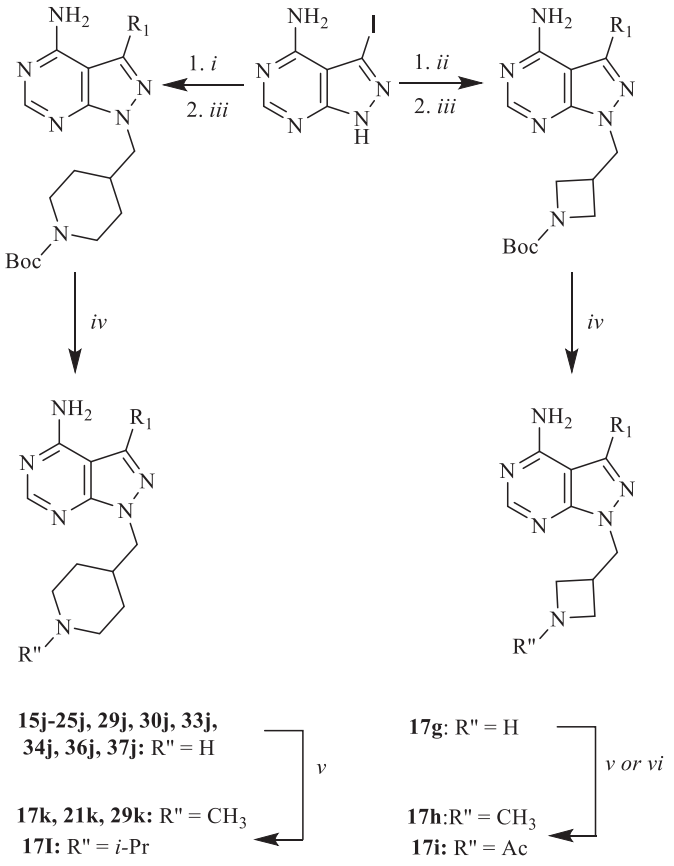

Scheme 3. General synthetic procedures for compounds with 4-azetidinemethylene and 4-piperidinemethylene substituents. *i*) *N*-Boc-4-piperidinemethanol mesylate, Cs_2CO_3, DMF, 80 °C; *ii*) *N*-Boc-3-azetidinemethanol mesylate, Cs_2CO_3, DMF, 80 °C; *iii*) Na_2CO_3, $Pd(PPh_3)_4$, boronic acid or boronate pinacol ester, H_2O/DME, 80 °C in microwave; *iv*) TFA/CH_2Cl_2 (1:1); *v*) sodium methoxide in MeOH, then 2% AcOH, R″-aldehyde, $NaBH_3CN$; *vi*) Ac_2O, TEA, DMF.

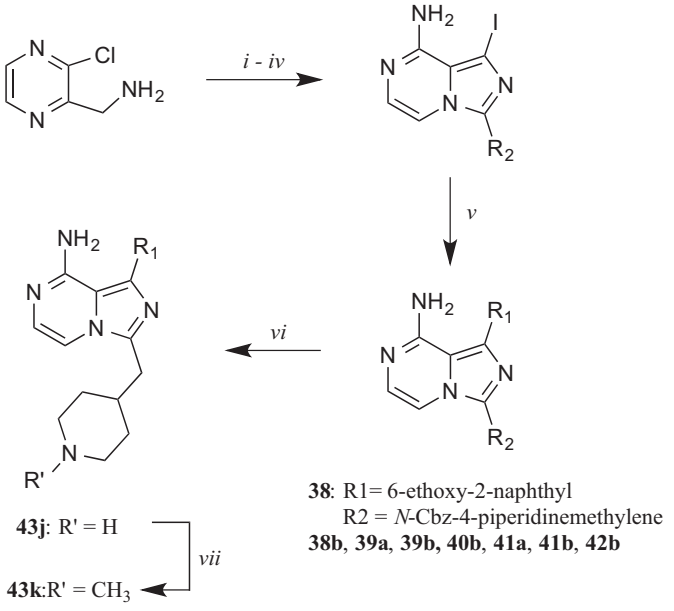

Scheme 4. General synthetic procedures for imidazo[1,5-*a*]pyrazine inhibitors. *i*) R_1CO_2H, EDCI, HOBt, CH_2Cl_2; *ii*) $POCl_3$, DMF (cat.), then TEA, CH_2Cl_2; *iii*) NIS, DMF; *iv*) NH_4OH, MeOH; *v*) Na_2CO_3, $Pd(PPh_3)_4$, boronic acid or boronate pinacol ester, H_2O/DME, 80 °C; *vi*) HCl (conc.); *vii*) CH_2O, $NaBH_3CN$.

pyridyl (**7a**), biphenyl (**13a**), and naphthylmethyl (**14a**), are not tolerated and show no appreciable enzyme inhibition at the highest concentration tested (3 μM). In general, inhibitors containing either 2-naphthyl or 6-quinilino substituents possess the greatest activity against *Pf*CDPK4, with 6-allyloxy-2-naphthyl (**24**) and 2-ethoxy-6-quinilino (**30**) substituents appearing to complement the ATP-binding site of this kinase most optimally; **24a** and **30a** demonstrate an IC_{50} of less than 20 nM. The extended hydrophobic surface of these substituents appear to make optimal interactions with the binding pocket next to the gatekeeper residue of *Pf*CDPK4, much like these same substituents are able to make extensive contact with the highly similar ATP-binding site of *Tg*CDPK1 [27].

Despite the ability of *Pf*CDPK4's ATP-binding site to favorably interact with a number of inhibitors, all of the analogs tested in Table 1 are more potent against glycine gatekeeper-containing *Tg*CDPK1, with 63% of the compounds in Table 1 displaying a >20-fold lower IC_{50} for *Tg*CDPK1 than *Pf*CDPK4. Thus, the enlarged ATP-binding pocket of *Tg*CDPK1 is better able to form favorable interactions with bulky C-3 substituents than the more constricted active site of *Pf*CDPK4. Interestingly, the slightly larger threonine gatekeeper residue of *Pf*CDPK1 does not alter inhibitor efficacy in the majority of cases. Of the inhibitors in Table 1 that were tested against both kinases, 67% differ in IC_{50} by less than 3-fold. However, several analogs that contain smaller 6-alkoxy-2-naphthyl and 2-alkoxy-6-quinilino C-3 substituents (**16a**, **17b**, **30a**, and **31a**) are >5-fold more potent against *Pf*CDPK4. In contrast, inhibitors that contain larger 6-alkoxy- and 6-benzyloxynaphthol groups (**21a**, **25a**, **26a**, **28a**, and **33a**) are >3-fold more potent against *Pf*CDPK1 than *Pf*CDPK4 (Table 1). Therefore, even small differences in the gatekeeper residue can result in varying sensitivities to inhibitors with large R_1 substituents.

Next, analogs that contain variable R_2 groups and 6-alkoxy-2-naphthyl or 2-alkoxy-6-quinilino substituents at the C-3 position (R_1) were tested (Table 2). The most comprehensive series of these analogs contain a 6-ethoxy-2-naphthyl R_1 group and variable R_2 substituents. Like *Tg*CDPK1, R_2 groups that contain functionalities that are connected to the *N*-1 position of the pyrazolopyrimidine scaffold through a methylene linkage are favored by *Pf*CDPK4 [28]. For example, **17k**, which contains an *N*-methylpiperidine attached to the core scaffold through a methylene linkage, is ~4-fold more potent than an analog (**17c**) that contains no spacer. Similarly, **17q**, which contains an *isobutyl* group at the R_2 position, is more than 30-fold more potent than its *i*-Pr analog **17a**. Overall, the most favorable R_2 substituent is a 4-piperidinylmethylene group (series **j**, Table 2), which results in a >100-fold increase in potency against *Pf*CDPK4 in the context of several R_1 substituents. The two most potent *Pf*CDPK4 inhibitors identified in this study (compounds **30j** and **37j**; IC_{50} = 2 nM) have a 4-piperidinylmethylene group at the R_2 position and either a 2-ethoxyquinoline (**30**) or 6-cyclopropyloxynaphthyl (**37**) group at the R_1 position. While other R_2 groups do not confer similar increases in potency as the piperidinylmethylene (**j**) group, several substituents increase inhibitor potency by over 10-fold compared to their corresponding *i*-Pr R_2 derivatives.

Much like the inhibitors shown in Table 1, almost all of the analogs in Table 2 are more potent against *Tg*CDPK1 than *Pf*CDPK4. However, the fold differences in IC_{50} for most inhibitors between these two kinases are much smaller, with several compounds (for example, **15j**, **16j**, and **29j**) essentially being equipotent. Thus, the ability of the R_2 position to interact favorably with the R_1 position to confer selectivity is even more pronounced in *Pf*CDPK4 than *Tg*CDPK1. The ability of optimal R_2 groups to confer increased potency seems to hold for threonine gatekeeper-containing *Pf*CDPK1 as well, although to a lesser degree. The presence of a 4-piperidinylmethylene (**j**) group increases the potency of inhibitors

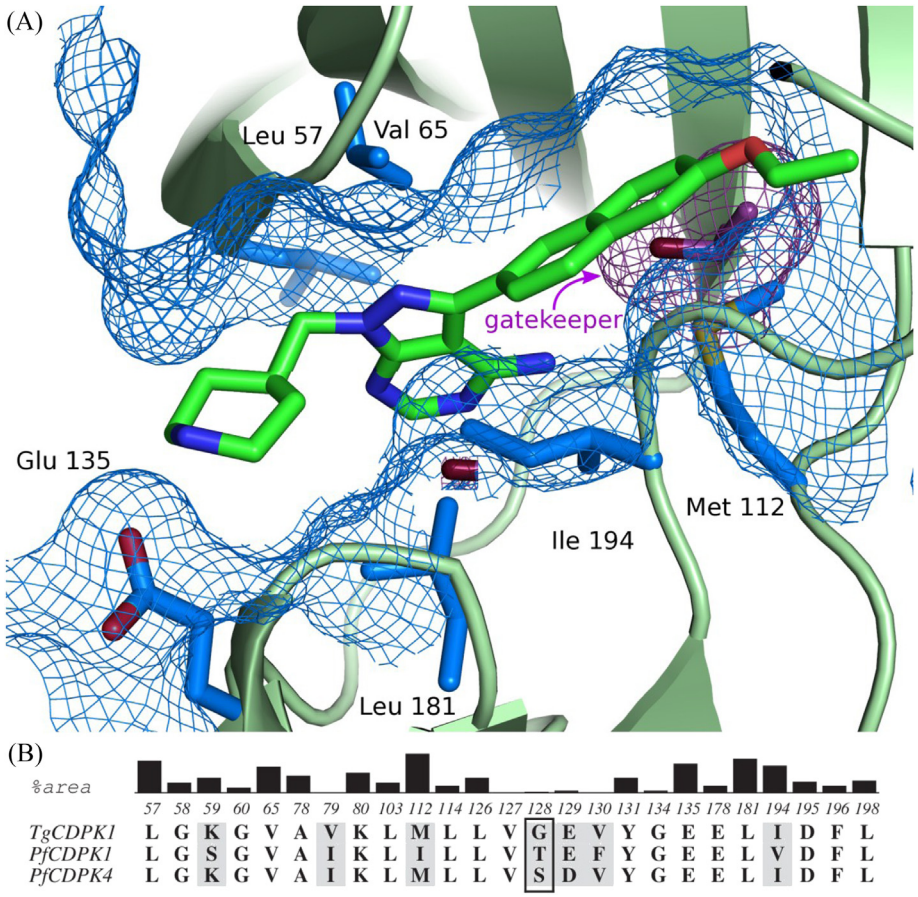

Fig. 2. (A) Structure of a pyrazolopyrimidine-based inhibitor (**17j**) bound to the ATP-binding site of *Tg*CDPK1. The six residues that contribute the largest surface area to the inhibitor binding site are show in blue. The gatekeeper residue is shown in purple. Residue numbering refers to that of *Tg*CDPK1. (B) Conservation of residues making up the CDPK active site. The residues shown are those within 5 Å of bound inhibitor **17j** as observed in complex with *Tg*CDPK1 (PDB 3sx9). The black vertical bars show the relative contributions of atoms in each reside to the surface area of the binding site in *Tg*CDPK1. Residues that are shaded gray are not conserved between *Tg*CDPK1, *Pf*CDPK1, and *Pf*CDPK4. The gatekeeper residue (Gly128 in *Tg*CDPK1 and Ser147 in *Pf*CDPK4) is boxed. (For interpretation of the references to color in this figure legend, the reader is referred to the web version of this article.)

that contain a 2-ethoxynaphthyl group (**17**) by ~10-fold relative to the *i*-Pr-containing analog. Several other R_2 groups that contain methylene linkages also increase potency by 10-fold or more. However, favorable R_2 groups will not allow 6-alkoxy-2-naphthyl and 2-alkoxy-6-quinilino C-3 substituents to be accommodated in CDPKs with every gatekeeper residue. A *Pf*CDPK4 mutant with a methionine gatekeeper residue (*Pf*CDPK4 S147M) is not sensitive to any of the compounds tested against it (**15j**, **17j**, **17q**, **30j**, **30u** and **37j**; Table 4).

Beyond varying the R_1 and R_2 substituents of our *Pf*CDPK4-directed compounds, we also evaluated the contribution of the scaffold to overall inhibitor selectivity and potency. To do this, a series of derivatives that contain optimal R_1 and R_2 groups displayed from an imidazopyrazine core were generated (Table 3). The imidazo[1,5-*a*]pyrazine scaffold makes almost the exact same hydrophobic and hydrogen-bonding contacts as the pyrazolopyrimidine scaffold, and projects its R_1 and R_2 substituents into similar regions of the ATP-binding pockets of kinases. A number of potent and selective inhibitors of IGF1R based on the imidazopyrazine core have previously been reported [33,34]. As expected, similar combinations of R_1 and R_2 substituents generally confer similar inhibitory activity against *Pf*CDPK4, independent of the scaffold. For example, the pyrazolopyrimidine-based (**17a**, Table 1) and imidazopyrazine-based (**43a**, Table 3) inhibitors that contain a 6-ethoxynapthyl (**17**) R_1 and *i*-Pr (**a**) R_2 groups have almost the same IC_{50}s against *Pf*CDPK4. The main exceptions to this trend are inhibitors that contain 4-piperidinemethylene (**j**) R_2 groups. Pyrazolopyrimidine-based inhibitors that contain this R_2 substituent are generally more potent than their corresponding imidazopyrazine analogs. This is

Table 4
Enzymatic assay (IC_{50}) results for *Pf*CDPK4 wt, a methionine gatekeeper mutant of *Pf*CDPK4 (Ser147Met), and the human tyrosine kinase Abl. *P. falciparum* gametocyte exflagellation inhibition (EC_{50}) and growth inhibition (GI_{50}) of human cell lines. All results are the averages of at least three assays. N/T = not tested.

	*Pf*CDPK4 IC_{50} (μM)	*P. falciparum* exflagellation inhibition EC_{50} (μM)	Abl IC_{50} (μM)	S147M *PfCDPK4* IC_{50} (μM)	HEPG2 GI_{50} (μM)	CRL8155 GI_{50} (μM)
15j	0.015	0.048	>10	>3	N/T	>30
17j	0.004	<0.040	>10	>3	>30	>30
17q	0.014	<0.040	2.7	>3	>30	>30
30j	0.002	<0.040	>10	>3	>30	>30
30u	0.004	<0.040	>10	>3	>30	>30
37j	0.002	<0.040	>10	>3	>30	>30

most likely due to a slight variation in the relative presentation of the R_1 and R_2 substituents from both scaffolds, which we have found to be important for the selectivity and potency of inhibitors that contain bulkier R_2 groups [28].

2.5. Pyrazolopyrimidine inhibitors with specific R_1 and R_2 substituent combinations are selective for PfCDPK4 over Src

While selectivity between threonine gatekeeper-containing-*Pf*CDPK1 and serine gatekeeper-containing-*Pf*CDPK4 provides information on how larger gatekeeper residues affect inhibitor potency in the context of almost identical ATP-binding sites, the main therapeutic liabilities of transmission-blocking kinase inhibitors are most likely off-target human kinases. To obtain a sense of target selectivity, a number of potent *Pf*CDPK4 inhibitors were tested against the mammalian tyrosine kinase Src. Prior studies have shown that some pyrazolopyrimidine-based inhibitors are able to potently inhibit Src kinase [36,37]. As the Src kinase gatekeeper position contains a threonine, which is one of the smallest gatekeeper residues in the human kinome, this enzyme was selected as a filter for off-target inhibition. A previously reported radioactive kinase assay was used to determine IC_{50} values for Src kinase [27].

The IC_{50}s of inhibitors that contain *i*-Pr (**a**) and *t*-Bu (**b**) R_2 groups are shown in the last column of Table 1. This inhibitor series clearly shows that it is challenging to obtain selectivity for *Pf*CDPK4 over Src based on the interaction of the R_1 substituent with the gatekeeper residue alone. Most aryl R_1 substituents provide near equipotent inhibition of *Pf*CDPK4 and Src, while inhibitors containing 6-benzyloxynaphthyl groups are selective for Src. However, a few R_1 groups, such as 1-methyl-5-benzimidazole (**11**), 6-methoxynaphthyl (**16**), 6-ethoxynaphthyl (**17**), and 2-ethoxyquinoline (**30**) confer greater than 10-fold selectivity for *Pf*CDPK4 over Src. Similar to our previous observations with *Tg*CDPK1, inhibitors that contain R_2 groups that are connected to the *N*-1 position of the pyrazolopyrimidine scaffold through a methylene linkage are significantly more selective for *Pf*CDPK4 than their *i*-Pr- and *t*-Bu-containing analogs [29,30]. For example, replacing the *t*-Bu R_2 group of inhibitor **17b** with a 4-azetidinemethylene (**17g**) or 4-piperidinemethylene (**17j**) group increases the selectivity for *Pf*CDPK4 over Src from ~30-fold to greater than 1300- and 5000-fold, respectively. This trend holds, regardless of the substituent displayed from the R_1 position. It should be noted that the observed increase in *Pf*CDPK4 selectivity is not only from increased potency against this enzyme, but also reduced affinity for Src. Therefore, like *Tg*CDPK1, the magnitude of selective inhibition of *Pf*CDPK4 over Src results from the interplay between the R_1 and R_2 substructures [30]. The ability of these analogs to potently inhibit *Pf*CDPK4 with minimal potency against Src points to the likelihood that with an optimal combination of R_1 and R_2 groups it should be possible to selectively target this kinase over potential mammalian off-target kinases. Consistent with this notion, inhibitors that are highly selective for *Pf*CDPK4 over Src show minimal inhibition of the human tyrosine kinase Abl (Table 4). Abl contains a threonine at the gatekeeper position and is also a likely off-target liability due to its sensitivity to pyrazolopyrimidine-based inhibitors [35].

2.6. Cellular activity of PfCDPK4 inhibitors

As an initial indicator of potential host cell toxicity of our transmission blocking compounds, we determined whether a number of potent *Pf*CDPK4 inhibitors block the growth of human liver (HepG2) and lymphocyte (CRL-8155) cell lines (Table 4). Assays were performed with a previously reported procedure [29]. All of the compounds tested show minimal growth inhibition at a concentration of 30 μM, which is consistent with the absence of off-target toxicity for this series of inhibitors.

We have previously demonstrated that when nanomolar concentrations of **17j** and **17k** are present in human blood containing *P. falciparum* gametocytes, microgamete exflagellation and infection of *Anopheles stephensi* is prevented [25,26]. In addition, a higher concentration of these drugs leads to the total absence of infective sporozoites in the dissected salivary glands of *A. stephensi*, with a lower dose still resulting in a significant decrease in observed sporozoites [25]. Importantly, intraperitoneal administration of **17j** to mice that are infected with *P. berghei* expressing *Pf*CDPK4 suppresses exflagellation in blood samples for up to 14 h post-injection [25]. The strong correlation between the ability of compounds to inhibit *Pf*CDPK4 *in vitro* and to block exflagellation strongly suggests that this effect is mediated through this kinase. Furthermore, *P. falciparum* expressing an exogenous drug-resistant *Pf*CDPK4 mutant [substitution of the serine gatekeeper residue with methionine] show decreased sensitivity to compound **17j** [26]. While several of our previously reported compounds show promising transmission blocking activity, we wanted to further demonstrate that potent *Pf*CDPK4 inhibitors with diverse functionalities have the potential to act as transmission blocking agents. To do this **17q**, **30u**, and **37j** were tested for their abilities to prevent *P. falciparum* exflagellation. All three of these inhibitors demonstrate an EC_{50} of less than 40 nM for parasite exflagellation. The efficacy of potent *Pf*CDPK4 inhibitors to block exflagellation further strengthens our hypothesis that our compounds are eliciting their effects through this enzyme. Moreover, the cellular efficacy of inhibitors with diverse functional groups allows greater flexibility in the optimization of the PK/ADME properties of transmission blocking compounds.

3. Conclusions

In the present study, we have profiled a number of pyrazolopyrimidine- and imidazopyrazine-based ATP-competitive inhibitors against a CDPK, *Pf*CDPK4, that is involved in parasite exflagellation. We found that it was possible to exploit similar interactions as our previous efforts to target *Tg*/*Cp*CDPK1, and that despite *Pf*CDPK4 possessing a larger serine gatekeeper residue, a number of these inhibitors possess low nanomolar potencies against this enzyme while retaining specificity against potential off-target human kinases. This is accomplished by exploiting the slightly enlarged pocket next to the serine gatekeeper residue of *Pf*CDPK4, in combination with an additional interaction in the ribose-binding pocket. The observed selectivity and potency of our *Pf*CDPK4 inhibitors carries over into cellular assays, where compounds potently inhibit *P. falciparum* exflagellation, but not the growth of human cell lines. Several compounds exhibit a large therapeutic window between inhibition of parasite exflagellation and human cell growth (e.g., >100–1000×). These inhibitors are undergoing additional testing to evaluate pharmacological properties such as solubility, pharmacokinetics, pharmacodynamics, and metabolism. Ideally, a compound would be given at the time of malaria therapy and would remain in the bloodstream for 3–4 weeks, the time it takes for gametocytes to be eliminated from humans after artemesinin combination therapy. Retention in the bloodstream for 3–4 weeks is necessary because it appears the effect on transmission is reversible, and the compound must be ingested with gametocytes to be effective [25]. Dosing at the time of antimalarial therapy is ideal, as it will be difficult, operationally, to ask people in endemic areas to take multiple doses at defined intervals to prevent transmission when they feel well. Only a few of our compounds have been tested to date in animal models, but they are cleared too quickly for 3–4 week persistence after co-

administration with antimalarial therapy. Thus, future studies will focus on decreasing clearance of the compounds, while retaining favorable oral bioavailability, efficacy, and non-toxic parameters. In addition, strategies for obtaining sustained drug release are also being explored. The results obtained here will direct these future studies to evaluate lead candidates in parasitic transmission models, in order to select a few compounds to undergo final pre-clinical drug development testing as malaria transmission-blocking agents.

4. Experimental procedures

4.1. General synthetic methods

Unless otherwise stated, all chemicals were purchased from commercial suppliers and used without further purification. Reaction progress was monitored by thin-layer chromatography on silica gel 60 F254 coated glass plates (EM Sciences). Chromatography was performed using an IntelliFlash 280 automated flash chromatography system, eluting on pre-packed Varian SuperFlash silica gel columns with hexanes/EtOAc or CH_2Cl_2/MeOH gradient solvent systems. For preparatory HPLC purification, samples were chromatographically separated using a Varian Dynamax Microsorb 100-5 C_{18} column (250 mm × 21.4 mm), eluting with H_2O/CH_3CN or H_2O/MeOH gradient solvent systems (+0.05% TFA). The purity of all final compounds was determined by two analytical RP-HPLC methods, using an Agilent ZORBAX SB-C_{18} (2.1 mm × 150 mm) or Varian Microsorb-MV 100-5 C_{18} column (4.6 mm × 150 mm), and eluting with either H_2O/CH_3CN or H_2O/MeOH gradient solvent systems (0.05% TFA) run over 30 min. Products were detected by UV at $\lambda = 254$ nm, with all final compounds displaying >95% purity. NMR spectra were recorded on Bruker 300 or 500 MHz spectrometers at ambient temperature. Chemical shifts are reported in parts per million (δ) and coupling constants in Hz. ^{1}H NMR spectra were referenced to the residual solvent peaks as internal standards (7.26 ppm for $CDCl_3$, 2.50 ppm for DMSO-d_6, and 3.34 ppm for CD_3OD). Mass spectra were recorded with a Bruker Esquire Liquid Chromatograph - Ion Trap Mass Spectrometer. Inhibitors were synthesized through several different routes, as represented in Schemes 1–3. Compound characterization data is presented in Supporting information.

4.2. Spectral data of compounds

4.2.1. 1-(4-(2-(4-Amino-3-(naphthalen-2-yl)-1H-pyrazolo[3,4-d]pyrimidin-1-yl)ethyl)piperidin-1-yl)ethanone (**15o**)

^{1}H NMR (301 MHz, DMSO-d_6): δ ppm 8.29 (s, 1H), 8.20 (s, 1H), 8.11–7.48 (m, 3H), 7.83 (dd, J = 8.5, 1.6 Hz, 1H), 7.63–7.56 (m, 2H), 4.42 (t, J = 6.8 Hz, 2H), 3.40 (m, 2H), 3.25 (m, 2H), 2.57 (m, 2H), 1.97 (s, 3H), 1.80 (m, 2H), 1.42 (m, 1H), 1.22 (m, 2H); MS (ESI): 415.4 m/z [MH+], $C_{24}H_{26}N_6O$ requires 415.2; HPLC-1 = 99.0% pure, HPLC-2 = 98.4% pure.

4.2.2. 1-(Naphthalen-2-yl)-3-((tetrahydro-2H-pyran-4-yl)methyl)-1H-pyrazolo[3,4-d]pyrimidin-4-amine (**15p**)

^{1}H NMR (300 MHz, DMSO-d_6): δ ppm 8.46 (s, 1H), 8.20 (s, 1H), 8.09 (d, J = 8.5 Hz, 1H), 8.02–7.94 (m, 2H), 7.80 (d, J = 8.5 Hz, 1H), 7.63–7.59 (m, 1H), 7.58–7.52 (m, 1H), 4.44 (d, J = 7.0 Hz, 2H), 4.02–3.92 (m, 2H), 3.47–3.35 (m, 2H), 2.37 (m, 1H), 1.65–1.53 (m, 2H), 1.53–1.40 (m, 2H); MS (ESI): 360.2 m/z [MH+], $C_{21}H_{21}N_5O$ requires 360.1; HPLC-1 = 96.0% pure, HPLC-2 = 97.0% pure.

4.2.3. 1-(Naphthalen-2-yl)-3-((acetylpiperazine-4-yl)ethanone)-1H-pyrazolo[3,4-d]pyrimidin-4-amine (**15t**)

^{1}H NMR (301 MHz, DMSO-d_6): δ ppm 8.26 (s, 1H), 8.21 (s, 2H), 7.99–8.04 (m, 3H), 7.82 (dd, J = 8.5, 1.6 Hz, 1H), 7.60 (m, 3H), 5.43 (d, J = 4.6 Hz, 2H), 3.71–3.54 (m, 4H), 3.54–3.40 (m, 4H), 2.08 (s, 3H); MS (ESI): 430.4 m/z [MH+], $C_{23}H_{23}N_7O_2$ requires 430.2; HPLC-1 = 97.8% pure, HPLC-2 = 97.6% pure.

4.2.4. 1-(Azetidin-3-ylmethyl)-3-(6-ethoxynaphthalen-2-yl)-1H-pyrazolo[3,4-d]pyrimidin-4-amine (**17g**)

^{1}H NMR (300 MHz, CD_3OD): δ ppm 8.52 (s, 1H), 8.17 (s, 1H), 8.00 (d, J = 8.3 Hz, 1H) 7.92 (d, J = 8.9 Hz, 1H), 7.79 (d, J = 8.5 Hz, 1H), 7.37 (s, 1H), 7.27 (d, J = 8.7 Hz, 1H), 4.84 (d, J = 6.4 Hz, 2H), 4.23 (m, 6H), 3.63 (m, 1H), 1.50 (t, J = 6.2 Hz, 3H); MS (ESI): 375.1 m/z [MH+], $C_{21}H_{22}N_6O$ requires 375.4; HPLC-1 = 96.1% pure, HPLC-2 = 97.0% pure.

4.2.5. 3-(6-Ethoxynaphthalen-2-yl)-1-((1-methylazetidin-3-yl)methyl)-1H-pyrazolo[3,4-d]pyrimidin-4-amine (**17h**)

^{1}H NMR (300 MHz, CD_3OD): δ ppm 8.50 (s, 1H), 8.15 (s, 1H), 8.00 (d, J = 8.5 Hz, 1H) 7.92 (d, J = 9.1 Hz, 1H), 7.77 (d, J = 8.2 Hz, 1H), 7.37 (d, J = 2.4 Hz, 1H), 7.27 (dd, J = 9.1, 2.4 Hz, 1H), 4.84 (q, J = 6.6 Hz, 2H), 4.45 (q, J = 6.2 Hz, 2H), 4.20 (m, 4H), 3.55 (m, 1H), 2.96 (s, 3H), 1.50 (t, J = 7.0 Hz, 3H); MS (ESI): 389.1 m/z [MH+], $C_{22}H_{24}N_6O$ requires 389.2; HPLC-1 = 97.0% pure, HPLC-2 = 97.5% pure.

4.2.6. 1-(3-((4-Amino-3-(6-ethoxynaphthalen-2-yl)-1H-pyrazolo[3,4-d]pyrimidin-1-yl)methyl)azetidin-1-yl)ethanone (**17i**)

^{1}H NMR (300 MHz, $CDCl_3$): δ ppm 8.38 (s, 1H), 8.06 (s, 1H), 7.92–7.70 (m, 3H) 7.25 (m, 2H), 5.70 (br s, 2H), 4.68 (d, J = 7.2 Hz, 2H), 4.18–3.97 (m, 6H), 3.29 (m, 1H), 1.86 (s, 3H), 1.51 (t, J = 7.0 Hz, 3H); MS (ESI): 417.4 m/z [MH+], $C_{23}H_{24}N_6O_2$ requires 417.4; HPLC-1 = 95.6% pure, HPLC-2 = 95.3% pure.

4.2.7. 3-(6-Ethoxynaphthalen-2-yl)-1-((1-isopropylpiperidin-4-yl)methyl)-1H-pyrazolo[3,4-d]pyrimidin-4-amine (**17l**)

^{1}H NMR (300 MHz, CD_3OD): δ ppm 8.46 (s, 1H), 8.13 (s, 1H), 7.97 (d, J = 7.8 Hz, 1H), 7.89 (d, J = 8.7 Hz, 1H), 7.77 (d, J = 8.2 Hz, 1H), 7.34 (s, 1H), 7.23 (d, J = 8.5 Hz, 1H), 4.51 (d, J = 6.2 Hz, 2H), 4.20 (q, J = 6.6 Hz, 2H), 3.48 (m, 2H), 3.05 (m, 3H), 2.44 (m, 1H), 2.01 (m, 2H), 1.76 (m, 2H), 1.48 (t, J = 6.8 Hz, 3H), 1.34 (d, J = 6.0 Hz, 6H); MS (ESI): 445.4 m/z [MH+], $C_{26}H_{32}N_6O$ requires 445.1; HPLC-1 = 95.0% pure, HPLC-2 = 97.5% pure.

4.2.8. 1-(4-(2-(4-Amino-3-(6-ethoxynaphthalen-2-yl)-1H-pyrazolo[3,4-d]pyrimidin-1-yl)ethyl)piperidin-1-yl)ethanone (**17o**)

^{1}H NMR (300 MHz, CD_3OD): δ ppm 8.34 (s, 1H), 7.97 (s, 1H), 7.88–7.73 (m, 2H), 7.62 (d, J = 8.5 Hz, 1H), 7.20 (s, 1H), 7.11 (d, J = 8.7 Hz, 1H), 4.41 (m, 3H), 4.09 (q, J = 6.8 Hz, 2H), 3.83 (m, 1H), 3.01 (m, 1H), 2.58 (m, 1H), 2.07 (s, 3H), 1.93–1.71 (m, 4H), 1.54–1.32 (m, 4H), 1.25–0.97 (m, 2H); MS (ESI): 459.2 m/z [MH+], $C_{26}H_{30}N_6O_2$ requires 459.2; HPLC-1 = 99.0% pure, HPLC-2 = 95.2% pure.

4.2.9. 3-(6-Ethoxynaphthalen-2-yl)-1-((tetrahydro-2H-pyran-4-yl)methyl)-1H-pyrazolo[3,4-d]pyrimidin-4-amine (**17p**)

^{1}H NMR (300 MHz, DMSO-d_6): δ ppm 8.28 (s, 1H), 8.12 (s, 1H), 7.96 (d, J = 8.7 Hz, 2H), 7.75 (d, J = 8.7 Hz, 1H), 7.41 (s, 1H), 7.23 (d, J = 9.6 Hz, 1H), 4.28 (d, J = 7.1 Hz, 2H), 4.20 (q, J = 6.8 Hz, 2H), 3.84 (m, 2H), 3.26 (m, 2H), 2.24 (m, 1H), 1.53–1.39 (m, 5H), 1.30 (m, 2H); MS (ESI): 404.3 m/z [MH+], $C_{23}H_{25}N_5O_2$ requires 404.1; HPLC-1 = 98.0% pure, HPLC-2 = 97.0% pure.

4.2.10. 3-(6-Ethoxynaphthalen-2-yl)-1-isobutyl-1H-pyrazolo[3,4-d]pyrimidin-4-amine (**17q**)

^{1}H NMR (300 MHz, CD_3OD): δ ppm 8.29 (s, 1H), 8.12 (s, 1H), 7.98 (d, J = 8.2 Hz, 1H), 7.92 (d, J = 9.1 Hz, 1H), 7.77 (dd, J = 8.7, 2.0 Hz, 1H), 7.35 (d, J = 2.4 Hz, 1H), 7.27–7.22 (dd, J = 9.1, 2.9 Hz, 1H), 4.29–4.18 (m, 4H), 2.40 (m, 1H), 1.50 (t, J = 6.8 Hz, 3H), 0.99 (d, J = 6.6 Hz,

6H); MS (ESI): 362.2 *m/z* [MH+], $C_{21}H_{23}N_5O$ requires 362.2; HPLC-1 = 96.3% pure, HPLC-2 = 97.2% pure.

*4.2.11. 1-(Cyclopropylmethyl)-3-(6-ethoxynaphthalen-2-yl)-1H-pyrazolo[3,4-d]pyrimidin-4-amine (**17r**)*

^{1}H NMR (300 MHz, CD_3OD): δ ppm 8.43 (s, 1H), 8.11 (s, 1H), 7.96 (d, *J* = 8.5 Hz, 1H), 7.88 (d, *J* = 9.1 Hz, 1H), 7.75 (d, *J* = 8.5 Hz, 1H), 7.32 (d, *J* = 2.0 Hz, 2H) 4.35 (d, *J* = 7.2 Hz, 2H), 4.20 (q, *J* = 6.8 Hz, 2H), 1.48 (m, 4H), 0.62 (m, 2H), 0.53 (m, 2H); MS (ESI): 360.2 *m/z* [MH+], $C_{21}H_{21}N_5O$ requires 360.2; HPLC-1 = 95.1% pure, HPLC-2 = 96.6% pure.

*4.2.12. 3-(6-(Cyclopropylmethoxy)naphthalen-2-yl)-1-isopropyl-1H-pyrazolo[3,4-d]pyrimidin-4-amine (**22a**)*

^{1}H NMR (300 MHz, CD_3OD): δ ppm 8.38 (s, 1H), 8.07 (s, 1H), 7.98–7.85 (m, 2H), 7.73 (d, *J* = 8.9 Hz, 1H), 7.29 (d, *J* = 8.7 Hz, 2H), 5.26 (m, 1H), 3.99 (d, *J* = 6.8 Hz, 2H), 1.67 (d, *J* = 6.6 Hz, 6H), 1.37 (m, 1H), 0.70 (q, *J* = 6.0 Hz, 2H), 0.44 (q, *J* = 4.7 Hz, 2H); MS (ESI): 374.3 *m/z* [MH+], $C_{22}H_{23}N_5O$ requires 374.1; HPLC-1 = 95.1% pure, HPLC-2 = 95.2% pure.

*4.2.13. 3-(6-(Cyclopropylmethoxy)naphthalen-2-yl)-1-(piperidin-4-ylmethyl)-1H-pyrazolo[3,4-d]pyrimidin-4-amine (**22j**)*

^{1}H NMR (300 MHz, CD_3OD): δ ppm 8.46 (s, 1H), 8.11 (s, 1H), 7.92 (m, 2H), 7.73 (s, 1H), 7.29 (s, 2H), 4.51 (d, *J* = 6.5 Hz, 2H), 3.99 (d, *J* = 6.8 Hz, 2H), 3.46 (m, 2H), 2.99 (m, 2H), 2.45 (m, 1H), 1.93 (m, 2H), 1.78 (m, 2H), 1.34 (m, 1H), 0.72 (m, 2H), 0.46 (m, 2H); MS (ESI) 429.4 *m/z* [MH+], $C_{25}H_{28}N_6O$ requires 429.2; HPLC-1 = 99.2% pure, HPLC-2 = 98.4% pure.

*4.2.14. 1-Isopropyl-3-(6-(2-methoxyethoxy)naphthalen-2-yl)-1H-pyrazolo[3,4-d]pyrimidin-4-amine (**23a**)*

^{1}H NMR (300 MHz, CD_3OD): δ ppm 8.42 (s, 1H), 8.11 (s, 1H), 7.85–8.04 (m, 2H), 7.77 (d, *J* = 8.2 Hz, 1H), 7.33 (s, 2H), 5.28 (m, 1H), 4.31 (t, *J* = 4.3 Hz, 2H), 3.88 (t, *J* = 4.5 Hz, 2H), 3.50 (s, 3H), 1.65 (d, *J* = 6.4 Hz, 6H); MS (ESI): 378.2 *m/z* [MH+], $C_{21}H_{23}N_5O_2$ requires 378.1; HPLC-1 = 95.0% pure, HPLC-2 = 95.4% pure.

*4.2.15. 1-((1-Methylpiperidin-4-yl)methyl)-3-(quinolin-6-yl)-1H-pyrazolo[3,4-d]pyrimidin-4-amine (**29k**)*

^{1}H NMR (300 MHz, CD_3OD): δ ppm 9.10 (d, *J* = 3.5 Hz, 1H), 8.82 (d, *J* = 8.2 Hz, 1H), 8.44 (m, 2H), 8.30 (m, 2H), 7.87 (dd, *J* = 8.2, 4.6 Hz, 1H), 4.51 (d, *J* = 4.6 Hz, 2H), 3.54 (m, 2H), 2.97 (t, *J* = 12.0 Hz, 2H), 2.84 (s, 3H), 2.40 (m, 1H), 1.98 (m, 2H), 1.69 (m, 2H); MS (ESI) 374.1 *m/z* [MH+], $C_{21}H_{24}N_7$ requires 374.2; HPLC-1 = 97.0% pure, HPLC-2 = 98.5% pure.

*4.2.16. 1-(4-(2-(4-Amino-3-(quinolin-6-yl)-1H-pyrazolo[3,4-d]pyrimidin-1-yl)ethyl)piperidin-1-yl)ethanone (**29o**)*

^{1}H NMR (301 MHz, DMSO-d_6): δ ppm 8.96 (d, *J* = 2.4 Hz, 1H), 8.50 (d, *J* = 8.2 Hz, 1H), 8.27 (m, 2H), 8.16 (d, *J* = 8.2 Hz, 1H), 8.06 (d, *J* = 8.5 Hz, 1H), 7.61 (dd, *J* = 8.5, 4.1 Hz, 1H), 4.45 (t, *J* = 6.5 Hz, 2H), 4.32–3.74 (m, 2H), 2.92 (m, 1H), 1.97 (s, 3H), 1.84 (m, 2H), 1.47 (m, 4H), 1.24–0.95 (m, 2H); MS (ESI): 416.4 *m/z* [MH+], $C_{23}H_{25}N_7O$ requires 416.1; HPLC-1 = 98.6% pure, HPLC-2 = 99.0% pure.

*4.2.17. 3-(2-Ethoxyquinolin-6-yl)-1-isopropyl-1H-pyrazolo[3,4-d]pyrimidin-4-amine (**30a**)*

^{1}H NMR (300 MHz, CD_3OD): δ ppm 8.68 (d, *J* = 8.9 Hz, 1H), 8.47 (s, 1H), 8.33 (s, 1H), 8.26–8.01 (m, 2H), 7.64 (m, 1H), 5.31 (m, 1H), 4.70 (q, *J* = 7.5 Hz, 2H), 1.64 (d, *J* = 6.2 Hz, 6H), 1.55 (t, *J* = 7.0 Hz, 3H); MS (ESI): 349.2 *m/z* [MH+], $C_{19}H_{20}N_6O$ requires 349.1; HPLC-1 = 98.0% pure, HPLC-2 = 95.0% pure.

*4.2.18. 3-(2-Ethoxyquinolin-6-yl)-1-((tetrahydro-2H-pyran-4-yl)methyl)-1H-pyrazolo[3,4-d]pyrimidin-4-amine (**30p**)*

^{1}H NMR (300 MHz, CD_3OD): δ ppm 8.45 (s, 1H), 8.35–8.01 (m, 2H), 7.98 (s, 1H), 7.67–7.47 (m, 1H), 7.07 (s, 1H), 4.55 (q, *J* = 6.8 Hz, 2H), 4.41 (m, 2H), 3.95 (d, *J* = 6.6 Hz, 2H), 3.40 (m, 2H), 2.35 (m, 1H), 1.58 (m, 2H), 1.51–1.41 (m, 5H); MS (ESI): 405.2 *m/z* [MH+], $C_{22}H_{24}N_6O_2$ requires 405.1; HPLC-1 = 98.0% pure, HPLC-2 = 97.0% pure.

*4.2.19. 3-(4-Amino-3-(2-ethoxyquinolin-6-yl)-1H-pyrazolo[3,4-d]pyrimidin-1-yl)-2,2-dimethylpropan-1-ol (**30u**)*

^{1}H NMR (300 MHz, CD_3OD): δ ppm 8.31 (s, 1H), 8.25 (d, *J* = 9.1 Hz, 1H), 8.14 (s, 1H), 7.99 (s, 2H), 7.03 (d, *J* = 9.1 Hz, 1H), 4.57 (q, *J* = 6.9 Hz, 2H), 4.35 (s, 4H), 1.49 (t, *J* = 7.3 Hz, 3H), 0.88 (s, 6H); MS (ESI): 393.2 *m/z* [MH+]; $C_{21}H_{24}N_6O_2$ requires 393.5; HPLC-1 = 95.2% pure, HPLC-2 = 98.0% pure.

*4.2.20. 3-(2-Ethoxy-8-methylquinolin-6-yl)-1-isopropyl-1H-pyrazolo[3,4-d]pyrimidin-4-amine (**31a**)*

^{1}H NMR (300 MHz, CD_3OD): δ ppm 8.26 (s, 1H), 8.20 (m, 1H), 7.93 (s, 1H), 7.83 (m, 1H), 6.98 (d, *J* = 8.9 Hz, 1H), 5.15 (m, 1H), 4.59 (q, *J* = 7.0 Hz, 2H), 1.60 (d, *J* = 6.6 Hz, 6H), 2.80 (s, 3H), 1.49 (t, *J* = 6.6 Hz, 3H); MS (ESI): 363.1 *m/z* [MH+], $C_{20}H_{22}N_6O$ requires 363.1; HPLC-1 = 95.0% pure, HPLC-2 = 96.0% pure.

*4.2.21. 3-(2-(Cyclopropylmethoxy)-8-methylquinolin-6-yl)-1-isopropyl-1H-pyrazolo[3,4-d]pyrimidin-4-amine (**32a**)*

^{1}H NMR (300 MHz, CD_3OD): δ ppm 8.44 (s, 1H), 8.06 (d, *J* = 8.9 Hz, 1H), 7.87 (s, 1H) 7.77 (s, 1H), 6.71 (d, *J* = 8.9 Hz, 1H), 5.27 (m, 1H), 3.45 (m, 2H), 2.63 (s, 3H), 1.70–1.60 (t, *J* = 6.6 Hz, 6H), 1.26–1.11 (m, 2H), 0.89 (m, 1H), 0.70–0.42 (m, 2H); MS (ESI): 389.6 *m/z* [MH+], $C_{22}H_{24}N_6O$ requires 389.2; HPLC-1 = 95.0% pure, HPLC-2 = 95.0% pure.

*4.2.22. 3-(2-(Benzyloxy)quinolin-6-yl)-1-isopropyl-1H-pyrazolo[3,4-d]pyrimidin-4-amine (**33a**)*

^{1}H NMR (300 MHz, CD_3OD) δ 8.42 (s, 1H), 8.27 (d, *J* = 8.9 Hz, 1H), 8.15 (d, *J* = 1.5 Hz, 2H), 8.04–7.95 (m, 2H), 7.54–7.49 (m, 2H) 7.41–7.31 (m, 2H), 7.10 (d, *J* = 8.9 Hz, 1H), 5.57 (s, 2H), 5.28 (m, 1H), 1.63 (d, *J* = 6.6 Hz, 6H); MS (ESI): 411.1 *m/z* [MH+], $C_{24}H_{22}N_6O$ requires 411.1; HPLC-1 = 95.0% pure, HPLC-2 = 99.0% pure.

*4.2.23. 3-(2-(Benzyloxy)quinolin-6-yl)-1-(piperidin-4-ylmethyl)-1H-pyrazolo[3,4-d]pyrimidin-4-amine (**33j**)*

^{1}H NMR (300 MHz, CD_3OD): δ ppm 8.26 (s, 1H), 8.21 (d, *J* = 8.9 Hz, 1H), 8.10 (s, 1H), 7.97 (s, 2H), 7.51 (d, *J* = 7.2 Hz, 2H), 7.41–7.29 (m, 3H), 7.06 (d, *J* = 8.7 Hz, 1H), 5.55 (s, 2H), 4.30 (d, *J* = 6.8 Hz, 2H), 3.03 (m, 2H), 2.55 (m, 2H), 2.19 (m, 1H), 1.60 (m, 2H), 1.35 (m, 2H); MS (ESI): 466.1 *m/z* [MH+], $C_{27}H_{27}N_7O$ requires 466.2; HPLC-1 = 95.0% pure, HPLC-2 = 98.2% pure.

*4.2.24. 3-(2-(Benzyloxy)-8-methylquinolin-6-yl)-1-isopropyl-1H-pyrazolo[3,4-d]pyrimidin-4-amine (**34a**)*

^{1}H NMR (300 MHz, $CDCl_3$): δ ppm 8.25 (s, 1H), 8.06 (d, *J* = 8.9 Hz, 1H), 7.84 (s, 1H), 7.75 (s, 1H), 7.57 (d, *J* = 8.0 Hz, 2H), 7.46–7.33 (m, 3H), 7.08 (d, *J* = 8.8 Hz, 1H), 5.62 (s, 2H), 5.28–5.15 (m, 1H), 2.81 (s, 3H), 1.66 (d, *J* = 6.7 Hz, 6H); MS (ESI): 425.2 *m/z* [MH+], $C_{25}H_{24}N_6O$ requires 425.2; HPLC-1 = 99.0% pure, HPLC-2 = 95.0% pure.

*4.2.25. 3-(2-(Benzyloxy)-8-methylquinolin-6-yl)-1-(piperidin-4-ylmethyl)-1H-pyrazolo[3,4-d]pyrimidin-4-amine (**34j**)*

^{1}H NMR (300 MHz, CD_3OD): δ ppm 8.27 (s, 1H), 8.20 (d, *J* = 8.7 Hz, 1H), 7.94 (s, 1H), 7.82 (s, 1H), 7.54 (d, *J* = 7.0 Hz, 2H), 7.35 (m, 3H), 7.06 (d, *J* = 8.9 Hz, 1H), 5.60 (s, 2H), 4.31 (d, *J* = 7.2 Hz, 2H), 3.05 (m, 2H), 2.77 (s, 3H), 2.57 (m, 2H), 2.20 (m, 1H), 1.63 (m, 2H),

1.35 (m, 2H); MS (ESI): 480.1 *m/z* [MH+], $C_{28}H_{29}N_7O$ requires 480.2; HPLC-1 = 95.5% pure, HPLC-2 = 95.0% pure.

*4.2.26. 1-(1-(Methylsulfonyl)piperidin-4-yl)-3-(quinolin-3-yl)-1H-pyrazolo[3,4-d]pyrimidin-4-amine (**35e**)*

^{1}H NMR (300 MHz, DMSO-d_6): δ ppm 9.26 (d, J = 2.0 Hz, 1H), 8.81 (s, 1H), 8.51 (s, 1H), 8.20 (dd, J = 7.4, 2.3 Hz, 1H), 7.94 (m, 2H), 7.78 (m, 1H), 4.99 (m, 1H), 3.75 (m, 2H), 3.07 (m, 2H), 2.96 (s, 3H), 2.26 (m, 2H), 2.14 (m, 2H); MS (ESI): 424.3 *m/z* [MH+]; $C_{20}H_{21}N_7O_2S$ requires 424.2; HPLC-1 = 97.8% pure, HPLC-2 = 98.0% pure.

*4.2.27. 1-(4-(4-Amino-3-(quinolin-3-yl)-1H-pyrazolo[3,4-d]pyrimidin-1-yl)piperidin-1-yl)ethanone (**35f**)*

^{1}H NMR (300 MHz, DMSO-d_6): δ ppm 9.17 (d, J = 2.1 Hz, 1H), 8.59 (d, J = 2.1 Hz, 1H), 8.30 (s, 1H), 8.11 (m, 2H), 7.83 (t, J = 8.5 Hz, 1H), 7.69 (t, J = 7.9 Hz, 1H), 5.04 (m, 1H), 4.55 (m, 1H), 4.00 (m, 1H), 3.40–3.33 (m, 2H), 2.80 (m, 1H), 2.20 (m, 1H), 2.07 (s, 3H), 1.99 (m, 2H); MS (ESI): 388.4 *m/z* [MH+], $C_{21}H_{21}N_7O$ requires 388.2; HPLC-1 = 99.5% pure, HPLC-2 = 99.2% pure.

*4.2.28. 3-(6-Cyclopropoxynaphthalen-2-yl)-1-(piperidin-4-ylmethyl)-1H-pyrazolo[3,4-d]pyrimidin-4-amine (**37j**)*

^{1}H NMR (300 MHz, CD_3OD): δ ppm 8.47 (s, 1H), 8.15 (s, 1H), 8.01 (d, J = 8.5 Hz, 1H), 7.91 (d, J = 9.1 Hz, 1H), 7.78 (d, J = 8.5 Hz, 1H), 7.62 (d, J = 2.0 Hz, 1H), 7.25 (dd, J = 8.9, 1.8 Hz, 1H), 4.50 (d, J = 6.0 Hz, 2H), 3.96 (m, 1H), 3.54 (m, 2H), 3.00 (m, 2H), 2.40 (m, 1H), 2.00 (m, 2H), 1.71 (m, 2H), 0.90 (m, 2H), 0.78 (m, 2H); MS (ESI): 415.1 *m/z* [MH+]; $C_{24}H_{26}N_6O$ requires 415.2; HPLC-1 = 95.5% pure, HPLC-2 = 97.2% pure.

*4.2.29. 1-(6-Ethoxynaphthalen-2-yl)-3-(piperidin-4-ylmethyl)imidazo[1,5-a]pyrazin-8-amine (**43j**)*

^{1}H NMR (500 MHz, CD_3OD): δ ppm 8.08 (s, 1H), 7.97 (d, J = 8.3 Hz, 1H), 7.87 (d, J = 8.7 Hz, 1H), 7.80 (d, J = 5.5 Hz, 1H), 7.70 (d, J = 7.6 Hz, 1H), 7.34 (s, 1H), 7.24 (d, J = 8.1 Hz, 1H), 7.02 (d, J = 5.5 Hz, 1H), 4.20 (q, J = 6.8 Hz, 2H), 3.41 (d, J = 10.0 Hz, 2H), 3.09 (m, 2H), 3.00 (m, 2H), 2.31 (m, 1H), 2.01 (m, 2H), 1.60 (m, 2H), 1.49 (t, J = 6.8 Hz, 3H); MS (ESI): 402.1 *m/z* [MH$^+$], $C_{24}H_{27}N_5O$ requires 402.2; HPLC-1 = 97.0% pure, HPLC-2 = 96.0% pure.

*4.2.30. 1-(6-Ethoxynaphthalen-2-yl)-3-((1-methylpiperidin-4-yl)methyl)imidazo[1,5-a]pyrazin-8-amine (**43k**)*

^{1}H NMR (500 MHz, CD_3OD): δ ppm 8.09 (s, 1H), 7.98 (d, J = 9.1 Hz, 1H), 7.89 (d, J = 9.1 Hz, 1H), 7.82 (d, J = 5.8 Hz, 1H), 7.72 (d, J = 8.9 Hz, 1H), 7.35 (s, 1H), 7.25 (d, J = 8.9 Hz, 1H), 7.03 (d, J = 5.8 Hz, 1H), 4.21 (q, J = 6.6 Hz, 2H), 3.53 (d, J = 10.0 Hz, 2H), 3.11 (m, 2H), 3.03 (m, 2H), 2.85 (s, 3H), 2.32 (m, 1H), 2.07 (m, 2H), 1.76–1.56 (m, 2H), 1.48 (t, J = 6.6 Hz, 3H); MS (ESI): 416.1 *m/z* [MH$^+$] $C_{25}H_{29}N_5O$ requires 416.2; HPLC-1 = 96.0% pure, HPLC-2 = 97.0% pure.

4.3. PfCDPK4 activity assays

The wild type and Ser147Met gatekeeper mutants of *Pf*CDPK4 were expressed, purified, and enzymatically characterized as described previously [25,26]. *Pf*CDPK4 activity assays were performed in assay buffer containing 20 mM HEPES (pH = 7.5), 0.1% BSA, 10 mM $MgCl_2$, 1 mM EGTA, 2 mM $CaCl_2$, 10 μM ATP, and 40 μM Syntide-2 peptide substrate (peptide sequence: PLARTLSVAGLPGKK-OH). After incubating for 90 min at 30 °C, the enzymatic reactions were terminated by adding EGTA [final concentration = 5 mM]. The amount of ATP remaining was evaluated using the Kinase Glo luciferase assay from Promega. Sample luminescence was determined using a Microbeta 2 plate reader (Perkin Elmer, Waltham, MA). Data were converted to percent inhibition and IC_{50} values were calculated with non-linear regression analysis using GraphPad Prism. All IC_{50} values shown are the average of assays that were performed in triplicate or quadruplicate.

4.4. Human kinase enzymatic assays

Compounds were tested for Src kinase inhibition using either the truncated catalytic kinase domain (Src-KD) or a construct that also contains Src's regulatory SH2 and SH3 domains (Src-3D). No significant difference in IC_{50} values was observed between the two constructs, and values are therefore reported together as Src kinase IC_{50}. Several compounds were further tested against Abl tyrosine kinase. For both Src and Abl, compounds were tested in 3-fold dilution series starting at an initial concentration of 10 μM according to previously reported procedures. Data were converted to percent inhibition and IC_{50} values were calculated with non-linear regression analysis using GraphPad Prism. All IC_{50} values shown are the average of assays that were performed in triplicate or quadruplicate. Assay buffers, enzyme concentrations, ATP concentrations, substrate peptide sequences and concentrations, and enzymatic reaction times are listed in the assay-specific details presented below.

Src assay buffer: recombinant Src-KD or Src-3D (1–2 nM), 33.5 mM HEPES, pH = 7.5, 6.7 mM $MgCl_2$, 1.7 mM EGTA, 67 mM NaCl, 2 mM Na_3VO_4, 0.08 mg/ml BSA, γ^{32}P ATP (0.2 μCi/well). Enzymatic reaction time: 30 min for Src-KD or 60 min for Src-3D. Substrate peptide sequence and concentration: Ac-EIYGEFKKK-OH (100 μM).

Abl assay buffer: recombinant Abl (1–2 nM), 33.5 mM HEPES, pH = 7.5, 6.7 mM $MgCl_2$, 1.7 mM EGTA, 67 mM NaCl, 2 mM Na_3VO_4, 0.08 mg/ml BSA, γ^{32}P ATP (0.2 μCi/well). Enzymatic reaction time: 30 min for Abl-KD and 60 min for Abl-3D. Substrate peptide sequence and concentration: Ac-EAIYAAPFAKKK-OH (100 μM).

4.5. Human cell growth inhibition assays

*Pf*CDPK4-selective compounds were tested for the growth inhibition of two human cell lines: HepG2 (liver) and CRL-8155 (lymphocytic) cells. Cells were grown in either DMEM/F12 (HepG2) or RPMI-1640 (CRL-8155) growth media supplemented with 10% heat inactivated fetal calf serum and 2 mM L-glutamine. HepG2 growth medium additionally contained 25 mM HEPES. CRL-8155 growth medium additionally contained 10 mM HEPES, 1 mM sodium pyruvate, 4.5 g/L glucose and 1.5 g/L sodium bicarbonate. Cells were grown in the presence of varying concentration of inhibitor (highest concentration = 30 μM; 3-fold dilution) for 48 or 72 h at 37 °C and 5% CO_2 in 96-well flat-bottom plates (Corning). Growth was quantified using Alamar Blue as a developing reagent and detecting sample absorbance at λ = 570 nm (600 nm reference wavelength). Percent growth inhibition by test compounds were calculated based on cultures incubated with DMSO negative and tipifarnib (R115777) positive controls (0% and 100% growth inhibition, respectively). All assays were performed in triplicate.

4.6. P. falciparum exflagellation assays

Cultures of wild-type *P. falciparum* that had been started at 0.5% were grown for 15 days in RPMI 1640 supplemented with 50 mM hypoxanthine and 10% A+ human serum, with daily media changes. Exflagellation was monitored beginning on day 14. After 15 days, the cultures were divided into flasks and varying concentrations of inhibitors or DMSO were added [25]. A wet mount slide was used for induction and monitoring of exflagellation. Parasites were monitored for exflagellation from 10 min to 25 min after exflagellation was induced. Exflagellation centers per 10,000 erythrocytes were counted.

Acknowledgment

The authors would like to thank Stephen Nakazawa Hewitt and DNAillustrated.com for designing and depicting the Plasmodium life cycle figure. The authors also acknowledge the helpful support of Lynn K. Barrett. Research reported in this publication was supported by the National Institute of Allergy and Infectious Diseases and the National Institute of General Medical Sciences of the National Institutes of Health under award numbers R01AI089441 and R01GM086858. K.R.K. was supported by a training scholarship from the University of Washington Plein Endowment for Geriatric Pharmacy Research. The content is solely the responsibility of the authors and does not necessarily represent the official views of the National Institutes of Health.

Appendix A. Supplementary data

Supplementary data related to this article can be found at http://dx.doi.org/10.1016/j.ejmech.2013.12.048.

References

[1] W.H. Organization, World Malaria Report 2010, 2010. Geneva.
[2] R. Carter, K.N. Mendis, Evolutionary and historical aspects of the burden of malaria, Clin. Microbiol. Rev. 15 (2002) 564–594.
[3] R.W. Snow, C.A. Guerra, A.M. Noor, H.Y. Myint, S.I. Hay, The global distribution of clinical episodes of *Plasmodium falciparum* malaria, Nature 434 (2005) 214–217.
[4] B.M. Greenwood, D.A. Fidock, D.E. Kyle, S.H. Kappe, P.L. Alonso, F.H. Collins, P.E. Duffy, Malaria: progress, perils, and prospects for eradication, J. Clin. Invest. 118 (2008) 1266–1276.
[5] S. Jongwutiwes, C. Putaporntip, T. Iwasaki, T. Sata, H. Kanbara, Naturally acquired *Plasmodium knowlesi* malaria in human, Thailand, Emerg. Infect. Dis. 10 (2004) 2211–2213.
[6] J. Cox-Singh, T.M.E. Davis, K.S. Lee, S.S.G. Shamsul, A. Matusop, S. Ratnam, H.A. Rahman, D.J. Conway, B. Singh, *Plasmodium knowlesi* malaria in humans is widely distributed and potentially life threatening, Clin. Infect. Dis. 46 (2008) 165–171.
[7] C.J.L. Murray, L.C. Rosenfeld, S.S. Lim, K.G. Andrews, K.J. Foreman, D. Haring, N. Fullman, M. Naghavi, R. Lozano, A.D. Lopez, Global malaria mortality between 1980 and 2010: a systematic analysis, Lancet 379 (2012) 413–431.
[8] J.F. Trape, A. Tall, N. Diagne, O. Ndiath, A.B. Ly, J. Faye, F. Dieye-Ba, C. Roucher, C. Bouganali, A. Badiane, F.D. Sarr, C. Mazenot, A. Toure-Balde, D. Raoult, P. Druilhe, O. Mercereau-Puijalon, C. Rogier, C. Sokhna, Malaria morbidity and pyrethroid resistance after the introduction of insecticide-treated bednets and artemisinin-based combination therapies: a longitudinal study, Lancet Infect. Dis. 11 (2011) 925–932.
[9] P. Schneider, T. Bousema, S. Omar, L. Gouagna, P. Sawa, H. Schallig, R. Sauerwein, (Sub)microscopic *Plasmodium falciparum* gametocytaemia in Kenyan children after treatment with sulphadoxine-pyrimethamine monotherapy or in combination with artesunate, Int. J. Parasitol. 36 (2006) 403–408.
[10] T. Bousema, C. Drakeley, Epidemiology and infectivity of *Plasmodium falciparum* and *Plasmodium vivax* gametocytes in relation to malaria control and elimination, Clin. Microbiol. Rev. 24 (2011) 377.
[11] T. Bousema, L. Okell, S. Shekalaghe, J.T. Griffin, S. Omar, P. Sawa, C. Sutherland, R. Sauerwein, A.C. Ghani, C. Drakeley, Revisiting the circulation time of *Plasmodium falciparum* gametocytes: molecular detection methods to estimate the duration of gametocyte carriage and the effect of gametocytocidal drugs, Malar. J. 9 (2010).
[12] P. Wilairatana, S. Krudsood, N. Tangpukdee, Appropriate time for primaquine treatment to reduce *Plasmodium falciparum* transmission in hypoendemic areas, Korean J. Parasitol. 48 (2010) 179–182.
[13] R.T. Eastman, S. Pattaradilokrat, D.K. Raj, S. Dixit, B.B. Deng, K. Miura, J. Yuan, T.Q. Tanaka, R.L. Johnson, H.Y. Jiang, R.L. Huang, K.C. Williamson, L.E. Lambert, C. Long, C.P. Austin, Y.M. Wu, X.Z. Su, A class of tricyclic compounds blocking malaria parasite oocyst development and transmission, Antimicrob. Agents Chemother. 57 (2013) 425–435.
[14] P.L. Alonso, G. Brown, M. Arevalo-Herrera, F. Binka, C. Chitnis, F. Collins, O.K. Doumbo, B. Greenwood, B.F. Hall, M.M. Levine, K. Mendis, R.D. Newman, C.V. Plowe, M.H. Rodriguez, R. Sinden, L. Slutsker, M. Tanner, A research agenda to underpin malaria eradication, PLoS Med. 8 (2011).
[15] M.J. Delves, Plasmodium cell biology should inform strategies used in the development of antimalarial transmission-blocking drugs, Future Med. Chem. 4 (2012) 2251–2263.
[16] K. Nagamune, L.D. Sibley, Comparative genomic and phylogenetic analyses of calcium ATPases and calcium-regulated proteins in the apicomplexa, Mol. Biol. Evol. 23 (2006) 1613–1627.
[17] C. Doerig, O. Billker, T. Haystead, P. Sharma, A.B. Tobin, N.C. Waters, Protein kinases of malaria parasites: an update, Trends Parasitol. 24 (2008) 570–577.
[18] O. Billker, S. Lourido, L.D. Sibley, Calcium-dependent signaling and kinases in apicomplexan parasites, Cell Host Microbe 5 (2009) 612–622.
[19] A.K. Wernimont, M. Amani, W. Qiu, J.C. Pizarro, J.D. Artz, Y.H. Lin, J. Lew, A. Hutchinson, R. Hui, Structures of parasitic CDPK domains point to a common mechanism of activation, Proteins 79 (2011) 803–820.
[20] N. Kato, T. Sakata, G. Breton, K.G. Le Roch, A. Nagle, C. Andersen, B. Bursulaya, K. Henson, J. Johnson, K.A. Kumar, F. Marr, D. Mason, C. McNamara, D. Plouffe, V. Ramachandran, M. Spooner, T. Tuntland, Y. Zhou, E.C. Peters, A. Chatterjee, P.G. Schultz, G.E. Ward, N. Gray, J. Harper, E.A. Winzeler, Gene expression signatures and small-molecule compounds link a protein kinase to *Plasmodium falciparum* motility, Nat. Chem. Biol. 4 (2008) 347–356.
[21] S. Sebastian, M. Brochet, M.O. Collins, F. Schwach, M.L. Jones, D. Goulding, J.C. Rayner, J.S. Choudhary, O. Billker, A Plasmodium calcium-dependent protein kinase controls zygote development and transmission by translationally activating repressed mRNAs, Cell Host Microbe 12 (2012) 9–19.
[22] J.D. Dvorin, D.C. Martyn, S.D. Patel, J.S. Grimley, C.R. Collins, C.S. Hopp, A.T. Bright, S. Westenberger, E. Winzeler, M.J. Blackman, D.A. Baker, T.J. Wandless, M.T. Duraisingh, A plant-like kinase in *Plasmodium falciparum* regulates parasite egress from erythrocytes, Science 328 (2010) 910–912.
[23] I. Siden-Kiamos, A. Ecker, S. Nyback, C. Louis, R.E. Sinden, O. Billker, *Plasmodium berghei* calcium-dependent protein kinase 3 is required for ookinete gliding motility and mosquito midgut invasion, Mol. Microbiol. 60 (2006) 1355–1363.
[24] O. Billker, S. Dechamps, R. Tewari, G. Wenig, B. Franke-Fayard, V. Brinkmann, Calcium and a calcium-dependent protein kinase regulate gamete formation and mosquito transmission in a malaria parasite, Cell 117 (2004) 503–514.
[25] K.K. Ojo, C. Pfander, N.R. Mueller, C. Burstroem, E.T. Larson, C.M. Bryan, A.M. Fox, M.C. Reid, S.M. Johnson, R.C. Murphy, M. Kennedy, H. Mann, D.J. Leibly, S.N. Hewitt, C.L. Verlinde, S. Kappe, E.A. Merritt, D.J. Maly, O. Billker, W.C. Van Voorhis, Transmission of malaria to mosquitoes blocked by bumped kinase inhibitors, J. Clin. Invest. 122 (2012) 2301–2305.
[26] K.K. Ojo, R.T. Eastman, R.S.R. Vidadala, Z. Zhang, K.L. Rivas, R. Choi, J.D. Lutz, M.C. Reid, A.M. Fox, M.A. Hulverson, M. Kennedy, N. Isoherranen, L.M. Kim, K.M. Comess, D.J. Kempf, C.L. Verlinde, X.Z. Su, S.H. Kappe, D.J. Maly, E. Fan, W.C. Van Voorhis, A specific inhibitor of PfCDPK4 blocks malaria transmission: chemical-genetic validation, J. Infect. Dis. 209 (2014) 275–284.
[27] K.K. Ojo, E.T. Larson, K.R. Keyloun, L.J. Castaneda, A.E. DeRocher, K.K. Inampudi, J.E. Kim, T.L. Arakaki, R.C. Murphy, L. Zhang, A.J. Napuli, D.J. Maly, C.L.M.J. Verlinde, F.S. Buckner, M. Parsons, W.G.J. Hol, E.A. Merritt, W.C. Van Voorhis, *Toxoplasma gondii* calcium-dependent protein kinase 1 is a target for selective kinase inhibitors, Nat. Struct. Mol. Biol. 17 (2010) 602–607.
[28] R.C. Murphy, K.K. Ojo, E.T. Larson, A. Castellanos-Gonzalez, B.G. Perera, K.R. Keyloun, J.E. Kim, J.G. Bhandari, N.R. Muller, C.L. Verlinde, A.C. White Jr., E.A. Merritt, W.C. Van Voorhis, D.J. Maly, Discovery of potent and selective inhibitors of calcium-dependent protein kinase 1 (CDPK1) from *C. parvum* and *T. gondii*, ACS Med. Chem. Lett. 1 (2010) 331–335.
[29] S.M. Johnson, R.C. Murphy, J.A. Geiger, A.E. DeRocher, Z.S. Zhang, K.K. Ojo, E.T. Larson, B.G.K. Perera, E.J. Dale, P.Q. He, M.C. Reid, A.M.W. Fox, N.R. Mueller, E.A. Merritt, E. Fan, M. Parsons, W.C. Van Voorhis, D.J. Maly, Development of *Toxoplasma gondii* calcium-dependent protein kinase 1 (TgCDPK1) inhibitors with potent anti-toxoplasma activity, J. Med. Chem. 55 (2012) 2416–2426.
[30] E.T. Larson, K.K. Ojo, R.C. Murphy, S.M. Johnson, Z.S. Zhang, J.E. Kim, D.J. Leibly, A.M.W. Fox, M.C. Reid, E.J. Dale, B.G.K. Perera, J. Kim, S.N. Hewitt, W.G.J. Hol, C.L.M.J. Verlinde, E. Fan, W.C. Van Voorhis, D.J. Maly, E.A. Merritt, Multiple determinants for selective inhibition of apicomplexan calcium-dependent protein kinase CDPK1, J. Med. Chem. 55 (2012) 2803–2810.
[31] Y. Liu, A. Bishop, L. Witucki, B. Kraybill, E. Shimizu, J. Tsien, J. Ubersax, J. Blethrow, D.O. Morgan, K.M. Shokat, Structural basis for selective inhibition of Src family kinases by PP1, Chem. Biol. 6 (1999) 671–678.
[32] C.E. Bulawa, M. Devit, D. Elbaum, Modulation of Protein Trafficking, WO2009062118A, 2009.
[33] M.J. Mulvihill, Q.S. Ji, D. Werner, P. Beck, C. Cesario, A. Cooke, M. Cox, A. Crew, H.Q. Dong, L.X. Feng, K.W. Foreman, G. Mak, A. Nigro, M. O'Connor, L. Saroglou, K.M. Stolz, I. Sujka, B. Volk, Q.H. Weng, R. Wilkes, 1,3-Disubstituted-imidazo [1,5-*a*]pyrazines as insulin-like growth-factor-I receptor (IGF-IR) inhibitors, Bioorg. Med. Chem. Lett. 17 (2007) 1091–1097.
[34] M.J. Mulvihill, Q.S. Ji, H.R. Coate, A. Cooke, H.Q. Dong, L.X. Feng, K. Foreman, M. Rosenfeld-Franklin, A. Honda, G. Mak, K.M. Mulvihill, A.I. Nigro, M. O'Connor, C. Pirrit, A.G. Steinig, K. Siu, K.M. Stolz, Y.C. Sun, P.A.R. Tavares, Y. Yao, N.W. Gibson, Novel 2-phenylquinolin-7-yl-derived imidazo[1,5-*a*] pyrazines as potent insulin-like growth factor-I receptor (IGF-IR) inhibitors, Bioorg. Med. Chem. 16 (2008) 1359–1375.
[35] J. Bain, L. Plater, M. Elliott, N. Shpiro, C.J. Hastie, H. McLauchlan, I. Klevernic, J.S. Arthur, D.R. Alessi, P. Cohen, The selectivity of protein kinase inhibitors: a further update, Biochem. J. 408 (2007) 297–315.
[36] J.H. Hanke, J.P. Gardner, R.L. Dow, P.S. Changelian, W.H. Brissette, E.J. Weringer, K. Pollok, P.A. Connelly, Discovery of a novel, potent, and Src family-selective tyrosine kinase inhibitor – study of Lck- and FynT-dependent T cell activation, J. Biol. Chem. 271 (1996) 695–701.
[37] K.R. Brandvold, M.E. Steffey, C.C. Fox, M.B. Soellner, Development of a highly selective c-Src kinase inhibitor, ACS Chem. Biol. 7 (2012) 1393–1398.